Journal of Applied Polymer Science

Rheology and Morphology of Polyester/Thermoplastic Flour Blends

Florian Démé,* Edith Peuvrel-Disdier, Bruno Vergnes
MINES ParisTech, CEMEF-Centre de Mise en Forme des Matériaux, Unité Mixte de Recherche Centre National de la Recherche Scientifique/Ecole des Mines 7635, CS 10207, 06904 Sophia Antipolis Cedex, France
*Present address: Laboratoire de Recherches et de Contrôle du Caoutchouc et des Plastiques, 60 Rue Auber, 94408 Vitry sur Seine Cedex, France
Correspondence to: E. Peuvrel-Disdier (E-mail: edith.disdier@mines-paristech.fr)

ABSTRACT: Two maize flours (standard and waxy grades) were plasticized in an internal mixer with a constant amount of water and two glycerol contents. The resulting thermoplastic flours (TPFs) were characterized in dynamic oscillatory shear and creep/recovery rheometry. They displayed two different behaviors: the viscoelastic behavior of a high-molecular-weight polymer for the first one and a gel-like behavior for the second one. The TPFs were then mixed with a copolyester [poly(butylene adipate–terephtalate)]. All of the blends contained the same volume fractions and were prepared with the same mixing conditions. The morphology and rheological behavior of each blend were characterized. Different morphologies, ranging from cocontinuous to nodular, were observed. In fixed mixing conditions, the blend morphology was shown to be governed by the rheological behavior of the starchy phase and the plasticizer content. The gel-like behavior of the second TPF seemed to prevent droplet coalescence; this led to a very fine dispersion. The rheological behavior of each blend appeared to be linked to both the morphology and the rheological behavior of the two phases.
 J. Appl. Polym. Sci. **2014**, *131*, 40222.

KEYWORDS: blends; biopolymers & renewable polymers; morphology; polyesters; rheology

Received 31 May 2013; accepted 17 November 2013
DOI: 10.1002/app.40222

INTRODUCTION

The development of polymer/thermoplastic starch (TPS) blends has recently widely increased, mainly for packaging applications.[1–4] A part of these studies has focused on synthetic polymer matrices, such as polyethylene (PE)[5–10] or polyamide.[11,12] However, the main part is devoted to bioplastics, such as poly(lactic acid),[13–17] polycaprolactone,[18–22] poly(butylene adipate–terephtalate) (PBAT),[23–26] or other aliphatic polyesters.[27–30] In some cases, ternary systems have also been studied.[16,25] Applications in areas such as films and bags require a fine dispersion of the starchy phase in the polymer matrix with sizes much smaller than the initial size of starch granules (5–20 μm). Indeed, the usual thickness of plastic films is around 10 μm. To reach this level of dispersion, it is necessary to destroy the native starch structure, either by fragmentation or by melting and dispersion. The second method is the most used. In this case, thermomechanical processing and plasticization of the starch phase is mandatory before it can be mixed with the polymer matrix.

The morphology of a polymer blend depends on the rheological properties of components (viscosity ratio and elasticity ratio), volume fractions, and interfacial tension.[31,32] To reduce the interfacial tension, it is common to add compatibilizers.[7,11,12,14,22,25]

Starch is composed of two polymer chains (amylose and amylopectin), which are both based on D-glucose units, and minor components such as lipids and traces of minerals.[33] Amylose is a linear chain, whereas amylopectin has a highly branched structure. The rheological behavior of thermoplastic starches is more complex than that of a classical polymer.[34–38] It depends on the starch botanical origins (more precisely, the ratio of amylose to amylopectin), eventual chemical modifications such as esterification, the amount and type of plasticizers, and the thermomechanical treatment undergone by the starchy phase during processing. Starch thermal transitions and phase transformations are also more complex than those of synthetic polymers. There are two main types of crystallinity for native starch. Three others, formed by amylose/lipid or amylose/glycerol complexes, appear during cooling, after the destruction of the native crystallinity during the process[39,40] and remain stable at high temperatures. Therefore, to prevent parasitic crystallization problems, it is common to plasticize starch in a first processing step and

then to mix it with the polymer phase without intermediate cooling.

Flour contains proteins in addition to starch. Its use in place of starch for preparing bioplastic blends is more rare. Therefore, the aim of this study was to characterize the behavior of two different thermoplastic flours (TPFs) during their mixing with a PBAT matrix. TPFs and blends were prepared in an internal batch mixer. The effect of the plasticizer amount was also studied through the comparison of two formulations. For a better understanding of the morphology and the rheological behavior of the blends, special attention was paid to the rheological characterization of the TPFs.

EXPERIMENTAL

Materials

Two maize flour types were kindly provided by ULICE (Riom, France): a waxy maize flour (which we called flour A) and a standard maize flour (which we called flour B). They differed essentially in their amylose/amylopectin ratio. The standard grade (flour B) contained 70% amylose and 30% amylopectin, whereas the waxy grade (flour A) only contained amylopectin. In addition to starch, the flours also contained proteins, lipids, and some minerals in small quantities (<1%).

Glycerol was chosen as a plasticizer. Two contents were selected: 15 and 30 wt %. These contents were based on the total weight of the TPF formula: Glycerol + Water + Flour. Indeed, to facilitate processing, water was also added to reach a total water content of 20 wt % (including the water initially present in the flour) for all formulations.

PBAT (kindly provided by ULICE) is a semicrystalline random copolymer with a crystallinity around 10%. Its comonomer units are butylene adipate and butylene terephthalate.

Processing

The TPFs and blends were processed with an internal mixer (Haake Rheocord 600P, ThermoFischer, Karlsruhe, Germany). Flour, water, and glycerol were initially mixed by hand and allowed to rest under controlled humidity conditions for 24 h before their introduction into the internal mixer. The mixing parameters were kept constant for all of the experiments: chamber temperature = 125°C, filling ratio = 70%, rotation speed = 175 rpm, and mixing time = 8 min. After this treatment, part of the flour was removed for further analysis, and the remaining part was blended with PBAT under the same mixing conditions. The PBAT/TPF weight ratio was kept constant, with PBAT forming the major phase. The exact PBAT/TPF ratio could not be indicated for confidentiality reasons, but it was in the range 60–80 wt % for the PBAT phase and 40–20 wt % for the TPFs.

For sake of simplicity, the TPF with flour A and 30 wt % glycerol content is denoted as TPF A30, and the corresponding PBAT/TPF blend is called A30 blend. Similar notations are used for the other products i.e. TPF A15, TPF B15, TPF B30, A15 blend, B15 blend and B30 blend.

Characterization

The TPF samples were quenched in liquid nitrogen, and cryofractures were observed by scanning electron microscopy (SEM) with a Philips XL30 ESEM with an accelerating voltage of 15 keV in backscattered-electron mode. These pictures, made under a low vacuum (0.1–1 mPa), were used to characterize the starch plasticization state.

The cryofractured TPF/PBAT blend surfaces were treated to dissolve either the starchy phase or the PBAT phase: attack in 1*N* sulfuric acid for 3 h under magnetic stirring to dissolve the starchy phase or dissolution of the PBAT phase in a 50/50 acetonitrile–chloroform mixture for 3 h at 50°C followed by centrifugation to collect the starchy phase. The samples were then metallized by vacuum plasma deposition of Au–Pd alloys before SEM observations.

The dynamic rheological behavior of the PBAT, TPF, and blends was characterized on a strain-controlled rheometer (ARES, TA Instruments). The measurements were carried out with parallel plates 25 mm in diameter and with a 1.5 mm gap. The samples were obtained by compression molding for 10 min at 20 MPa and 150°C, followed by cooling under pressure. The sample edges were coated with a thin film of silicone oil to limit water loss during the measurements. Striated plates were used to prevent wall slippage.

Creep/recovery measurements with a stress-controlled rheometer (Stresstech, Reologica) were also performed with the same protocol.

RESULTS

TPF Characterization

The specific mechanical energy (SME) provided during the TPF plasticization process was calculated from the time integration of the mixer torque. The SME values and final product temperatures are reported in Table I for the different TPFs (with the same mixing conditions). The SME values were different for the two flours and mainly depended on the plasticizer amount. The SME value for the TPF with the lowest glycerol content (15 wt %) was indeed three times larger than the one with the highest content (30 wt %). This was valid for both flour types. The SME values for the standard flour grade TPF B were in all cases higher than those for the waxy flour grade TPF A; this indicated a more viscous material. This higher viscosity also led to a higher overheating: compared to the chamber temperature (125°C), product temperatures up to 152°C were reached in TPF B15 after 8 min compared to those of 130–132°C for all other samples. The SEM pictures (not shown here) indicated that the presence of residual granules (or fragments) was fairly low for both flours, even though TPF B showed a few more residual particles.

Before characterizing the TPF rheological behavior, we evaluated their thermal stability with time sweep tests at 1 rad/s and

Table I. SME During TPF Processing and Final Product Temperatures

	Glycerol	
	15 wt %	30 wt %
Flour A	111 kWh/t, 132°C	38 kWh/t, 130°C
Flour B	228 kWh/t, 152°C	67 kWh/t, 132°C

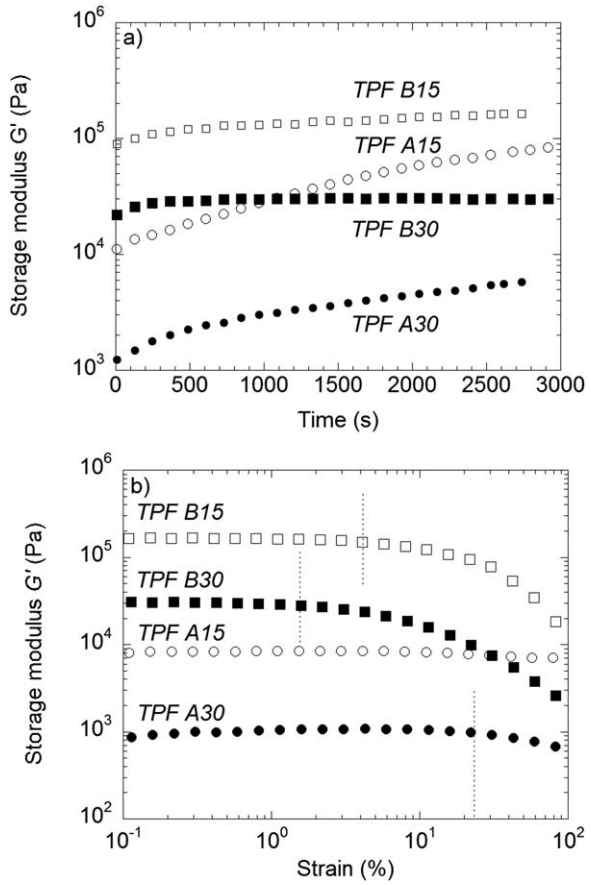

Figure 1. (a) Thermal stability (G' as a function of time at 1 rad/s and 1% strain) and (b) linear domain (G' as a function of the strain at 1 rad/s) for the two TPFs at 150°C with two plasticizer contents.

150°C in the linear viscoelastic domain (1% strain). As shown in Figure 1(a), the TPF storage modulus (G') increased with time, even though TPF B was more stable than TPF A. As expected from the torque measurements in the mixer, TPF B (standard grade) was more viscous than TPF A (waxy grade). The time evolution could have been due to a loss of plasticizer during the measurements. To check this point, the mass losses were measured after 48 h at 130°C on samples taken just after mixing and then after 1 h at 150°C in the rheometer. As shown in Table II, the mass losses varied from 8 to 23% after mixing and from 3 to 18% after the rheological measurements. This confirmed that despite the silicon oil, part of the volatiles evaporated during these measurements. Complementary measurements of the glycerol content (performed at Ecole Nationale Supérieure de Chimie de Clermont-Ferrand France) showed that the mass losses were mainly due to water for temperatures below 200°C. Consequently, we considered that the measured losses corresponded to the amount of water present in the samples at the beginning and at the end of the thermal stability tests. This means that around 3–4 wt % of the water was evaporated for TPF B in comparison with 12–15 wt % of the water for TPF A. The greater stability of TPF B15 was thus probably due to its low water content after processing (Table II). Even though an equivalent water amount was initially introduced in flours A and B, TPF B15 was subjected to a much larger overheating than TPF A15 (see Table I), and this led to a higher water loss. In the case of 30 wt % glycerol content, the overheating was low and similar for both flours, and this resulted in similar water losses. However, TPF A30 lost much more water during the rheological test; this indicated that water appeared to be less bonded to the standard flour grade A than to the waxy flour grade B at the same temperature.

Table II. Weight Loss During 48 h at 130°C for Samples Before and After Thermal Stability Testing at 150°C

	Mass loss (%)			
	TPF A15	TPF B15	TPF A30	TPF B30
Before	13.6	7.9	22.8	22.0
After	3.1	5.3	8.0	17.8

The linear viscoelastic domain was determined for the different samples [Figure 1(b)]. It was different for each TPF. The linear domain was much smaller for TPF B than for TPF A. Moreover, whatever the flour, it decreased when the glycerol content was increased. The critical strains were 1.6, 4.1, 22.2, and more than 100% for TPF B30, TPF B15, TPF A30, and TPF A15, respectively. This difference could be explained by the difference in the rheological behavior between the two TPFs.

Figure 2 presents the viscoelastic data [G', loss modulus (G''), and complex viscosity (η^*) vs frequency] for TPF A30 and TPF B30 at 150°C (similar results were obtained for the TPFs with 15 wt % glycerol but with higher values). TPF A30 showed a quasi-superposition of both modules over several decades; this was characteristic of a polymer melt of very high molecular weight with a branched structure.[41,42] This behavior was consistent with the composition of the waxy flour (100% amylopectin). η^* obeyed a power law with an index of 0.46. Conversely, TPF B30 exhibited a gel-like behavior with G' higher than G'' over the whole range of frequencies, with both moduli being quite independent of frequency. η^* also obeyed a power law but with a very low index, close to 0.06; this confirmed the plastic-like behavior of TPF B30. Such rheological behaviors have already been reported for TPS with similar amylose/amylopectin ratios.[34,35]

To complete the rheological characterization, creep experiments were carried out at 150°C (at 100 Pa during 480 s), and this was followed by recovery [Figure 3(a)]. TPF A30 showed a certain deformation during creep, which was proportional to time like for a viscoelastic fluid. However, the recovery seemed nonexistent. Conversely, TPF B30 was much more difficult to deform: under the same stress, the strain after 480 s was only 0.017 compared to 265 for TPF A30. However, by imposing a stress ramp between 0.1 and 50 Pa, we observed, as shown in Figure 3(b), that TPF B30 was effectively deformed but to a smaller extent and only above a yield stress of around 1 Pa.

The η^* values of the different formulations are compared in Figure 4. As already seen, flour B led to a more viscous TPF than flour A, and, for both materials, the viscosity decreased with increasing glycerol content. All of the curves could be fitted by power laws, with indices of 0.41, 0.46, 0.16, and 0.06 for

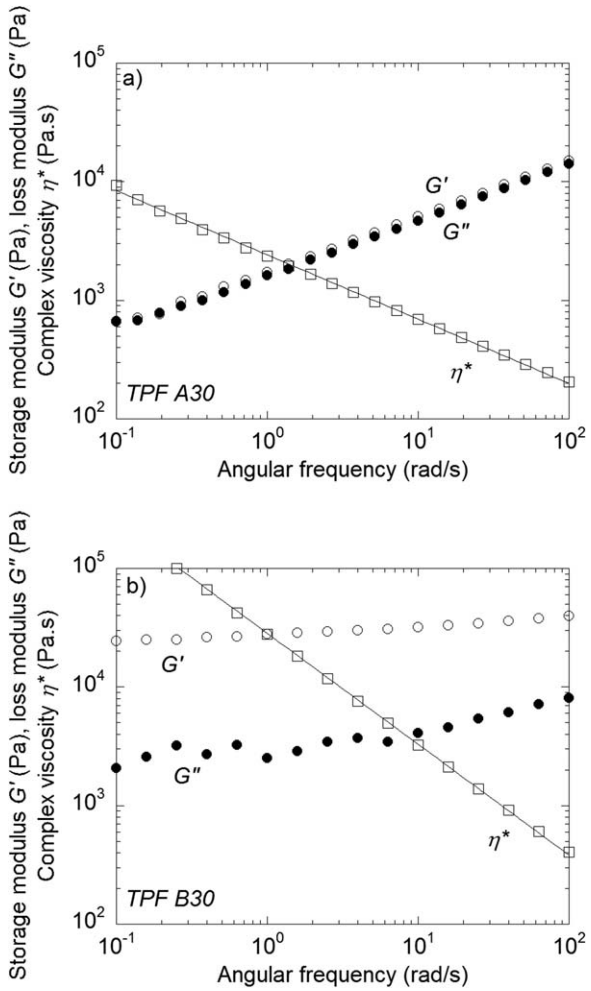

Figure 2. Viscoelastic moduli (G', G'') and η^* of TPF with 30 wt % glycerol as functions of the frequency at 150°C and 1% strain: (a) TPF A30 and (b) TPF B30.

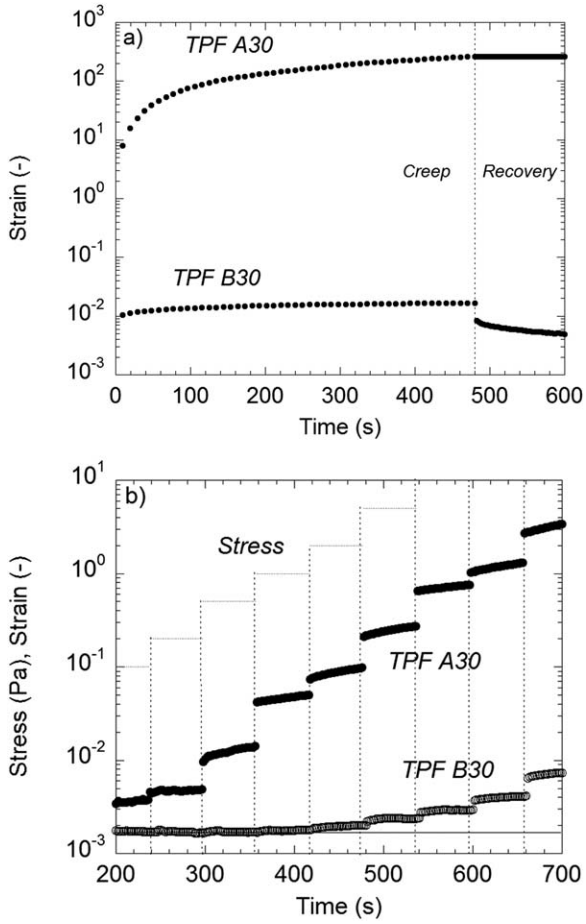

Figure 3. (a) Creep-recovery tests and (b) creep in stress steps for TPF A30 and TPF B30 at 150°C.

TPF A15, TPF A30, TPF B15, and TPF B30, respectively. The low power law index values for TPF B were coherent with the existence of a yield stress, as observed previously. The viscosity of the PBAT, which was used to prepare the blends discussed in the next section, is also indicated on the same figure for the sake of comparison. The PBAT viscosity was lower than that of both TPFs with 15 wt % glycerol. In the case of 30 wt % glycerol, depending on the frequency, the viscosity of PBAT was higher than those of both TPFs or between those of TPF B30 and TPF A30. We therefore expect to obtain different morphologies for the blends, depending on the glycerol content.

TPF/PBAT Blend Characterization

As for TPF, the SME provided to the blends during mixing, and the final product temperatures were recorded. The results are presented in Table III. In PBAT, which had a melting temperature that extended from 110 to 130°C, the starch phase underwent significant shear stresses at the beginning of mixing, and overheating was important. For a chamber temperature of 125°C, the final temperature of the blend reached 142–173°C. This temperature increase was slightly higher for blends with TPF B and more limited at a high glycerol content. The SME was generally high, between 170 and 563 kWh/t. The values were more important for blends based on TPF B and on the TPFs with low glycerol contents.

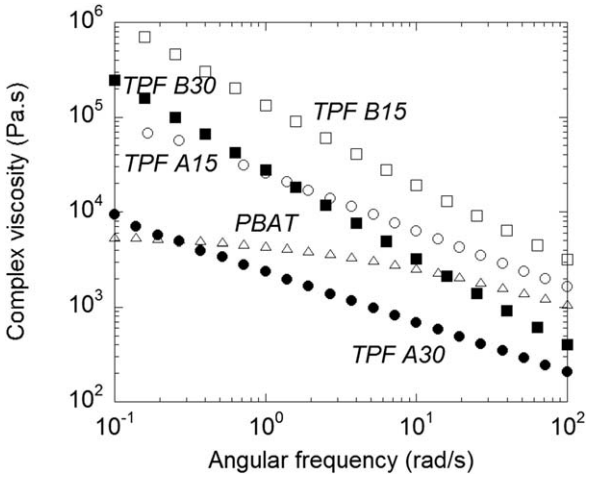

Figure 4. η^* as a function of the frequency at 150°C and 1% strain: (○) TPF A15, (□) TPF B15, (●) TPF A30, (■) TPF B30, and (△) PBAT.

Table III. SME During TPF/PBAT Mixing and Final Product Temperatures

	Glycerol in TPF	
	15 wt %	30 wt %
TPF A/PBAT blend	461 kWh/t, 169°C	170 kWh/t, 142°C
TPF B/PBAT blend	563 kWh/t, 173°C	398 kWh/t, 164°C

TPF/PBAT Blend Morphology. The PBAT/TPF blend morphologies were analyzed by SEM. Pictures for A15, A30, B15, and B30 blends are shown in Figures 5 and 6. A great diversity of both morphology and starchy phase size was observed. The blends realized with TPF A showed a relatively coarse morphology, with a nodular morphology for the A15 blend [spheres of several tens of micrometers, Figure 5(a,b)] and a cocontinuous one for the A30 blend [Figure 5(c,d)]. The cocontinuity of the A30 blend was more apparent, as shown in Figure 5(c), after dissolution of the starchy phase. Indeed, the starchy phase after PBAT extraction did not appear as continuous because it was very brittle. Nevertheless, the very large size of the starchy domains tended to confirm this assumption. Contrary to what could be expected from the rheological behavior, blends made with TPF B showed a much finer morphology with a nodular starchy phase (Figure 6). The nodules had a nice spherical shape. The average values of the nodule dimensions measured by image analysis are summarized in Table IV.

TPF/PBAT Blend Rheological Behavior. The thermal stability of the different TPF/PBAT blends was evaluated with time sweep tests at 1 rad/s and 150°C in the linear domain [1% strain; Figure 7(a)]. The presence of the PBAT matrix improved the thermal stability of the blend compared to TPF alone [Figure 1(a)]. However, it did not fully prevent water evaporation during the test. The blends based on TPF B were more stable, as was already noticed for the TPF B alone.

The linear viscoelastic domain was determined for all of the blends [Figure 7(b)]. It was almost the same for the different blends; the critical strain was around 10%, and it did not depend on the TPF type or glycerol content.

The linear viscoelastic behavior (G', G'', and η^* vs frequency) of the different blends is shown in Figure 8. Blend B15 presented classical viscoelastic behavior, with G'' larger than G' in the investigated range, a Newtonian plateau at a low frequency and a shear-thinning behavior at higher frequency. Blends A15 and A30 behaved similarly, with G'' larger than G' over the entire frequency range and a more pronounced shear-thinning behavior. The A15 blend tended to show at low frequency an onset of the

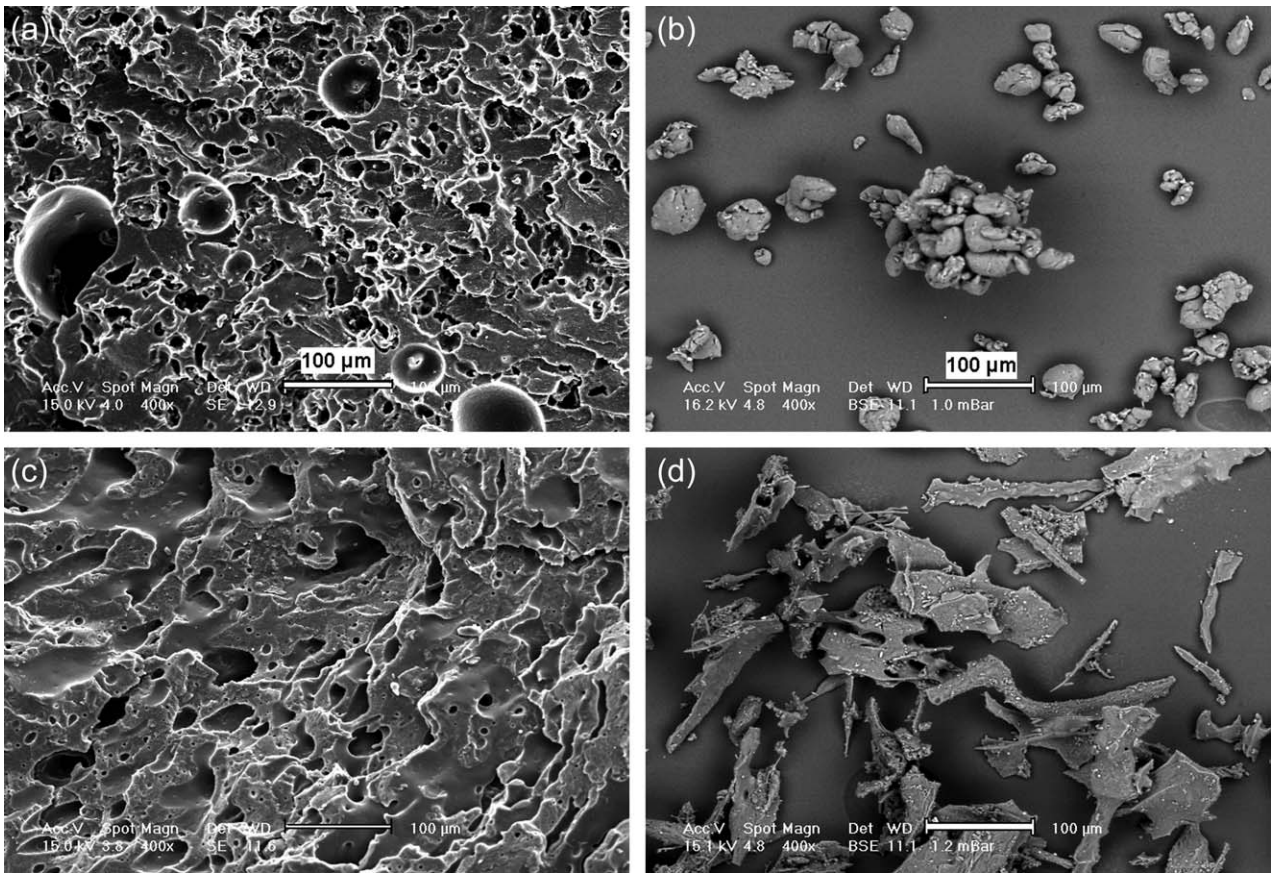

Figure 5. SEM micrographs of the A15 blend after the extraction of (a) the starchy phase and (b) PBAT and the A30 blend after the extraction of (c) the starchy phase and (d) PBAT.

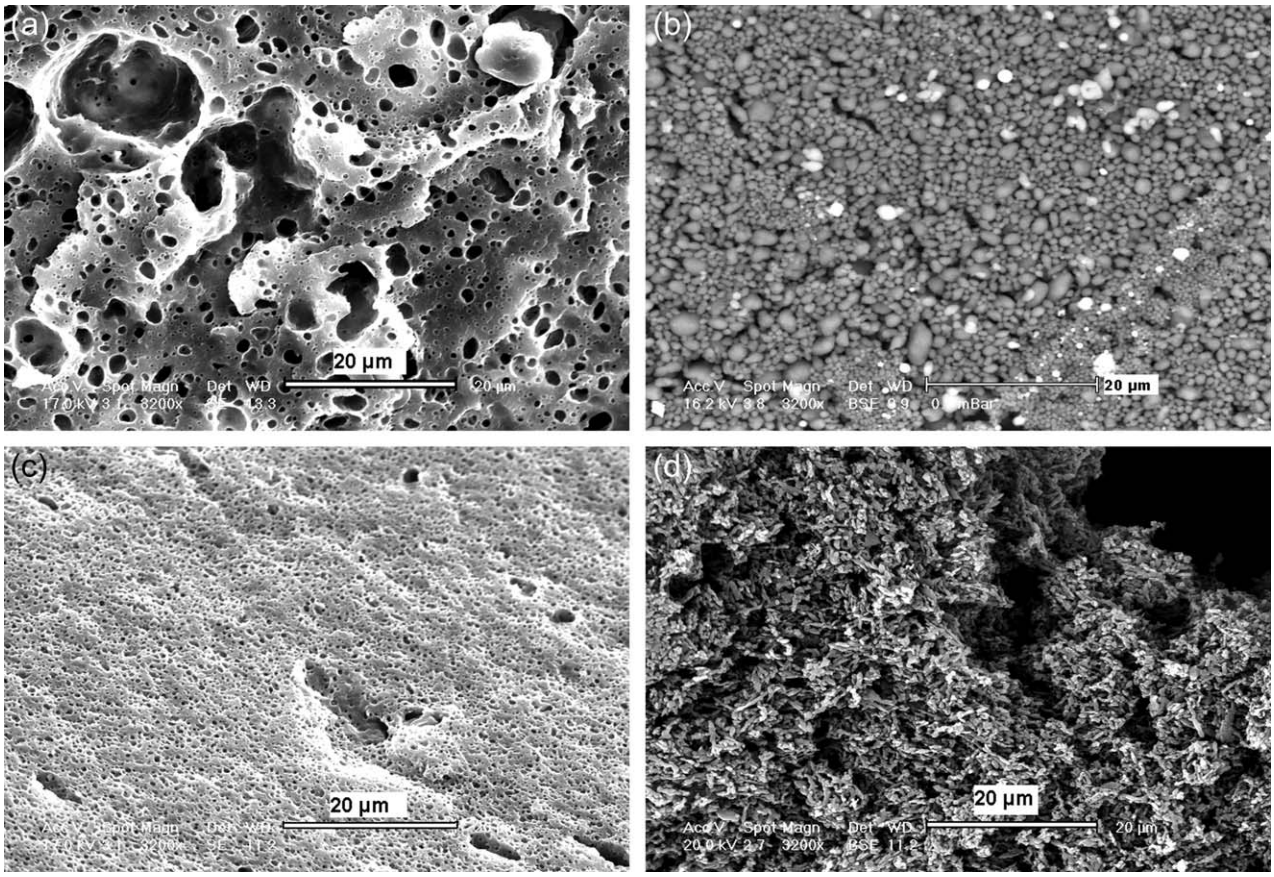

Figure 6. SEM micrographs of the B15 blend after the extraction of (a) the starchy phase and (b) PBAT and the B30 blend after the extraction of (c) the starchy phase and (d) PBAT.

G' plateau; this was associated with a low yield stress. The B30 blend depicted a different behavior, with G' quite superimposed with G'' over the investigated frequency range. The interpretation of these results, according to the behavior of the components and the blend morphology, is discussed in the next paragraph.

DISCUSSION

TPF/PBAT Blend Morphology

For a nodular morphology, the particle size is usually defined by the critical capillary number, which is a function of the ratio between the viscosity of the dispersed phase (Etad) and the one of the matrix (Etam).[43–45] Different expressions can be found in the literature, for simple (shear, elongation) or complex (extrusion) flow situations. For example, Wu[43] proposed the following empirical equation in the case of blends prepared by extrusion:

$$D = \frac{2\sigma}{\eta_m \dot{\gamma}} \left(\frac{\eta_d}{\eta_m}\right)^{\pm 0.84} \quad (1)$$

where D is the droplet diameter, σ is the interfacial tension, and $\dot{\gamma}$ is the shear rate. The exponent is positive for $\eta_d/\eta_m > 1$ and negative for $\eta_d/\eta_m < 1$. The η_d/ηm ratio must be calculated at the shear rate and product melt temperature corresponding to the processing conditions. This empirical model was established for blends of immiscible thermoplastic polymers. It considers that the droplet size results from an equilibrium between the interfacial stress and the shear stress and takes into account the effect of the viscosity ratio. It does not consider any effect of the components' elasticity on the blend morphology. Therefore, our purpose in the following was just to check whether the simple consideration of the viscosity ratio and the shear stress was enough to explain the variation in droplet size of the TPF/PBAT blends. In the internal mixer, the shear rate could be estimated from the rotor speed according to the methodology originally proposed by Bousmina et al.[46,47] At 175 rpm, the average shear rate was around 100 s^{-1}. Accordingly, the viscosity ratios were equal to 0.2 and 0.4 for the A30 and B30 blends and 1.5

Table IV. Blend Morphology and Medium Size (Length and Width) of the TPF Nodules

Blend	Morphology	Length (μm)	Width (μm)
A15	Nodular	21	12
A30	Cocontinuous	39	17
B15	Nodular	3.4	1.8
B30	Nodular	1.5	0.8

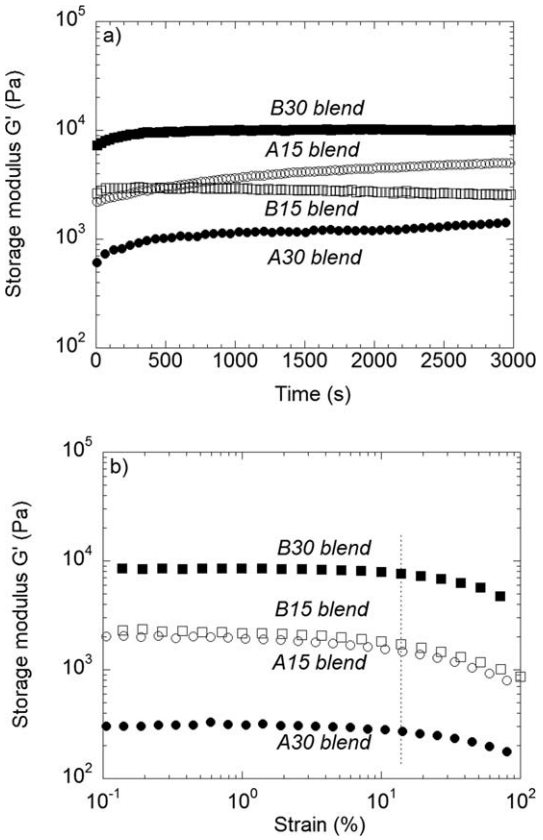

Figure 7. (a) Thermal stability (G' as a function of the time at 1 rad/s and 1% strain) and (b) linear domain (G' as a function of the strain at 1 rad/s) for the TPF/PBAT blends at 150°C.

and 3.0 for the A15 and B15 blends. If we assume that the nodule size follows eq. (1), the smallest size should be obtained for the A15 blend, the largest one should be obtained for the A30 blend, and similar values should be obtained for the B15 and B30 ones. As shown in Table IV, that was not really the case. This means that the viscosity ratio alone could not explain the size variations of the starchy phase. In addition to possible differences in the interfacial tension, the difference in the rheological behavior of the TPF phase was also at the origin of this size difference. Indeed, unlike TPF A, TPF B showed a gel-like behavior with a very short linear domain. This TPF was more elastic and could be deformed only under a high shear stress [Figure 3(b)]. Similar studies with modified highly elastic starches mixed with PE[6] or polycaprolactone[21] indicated that the deformed starch particles formed very stable fibrils because of their high elasticity. The gel-like behavior of TPF B could have also led to greater difficulties for particles to coalesce. Thus, this absence of coalescence explained the small nodule size observed in these blends, with deformation and rupture being the only possible mechanisms. In the case of TPF A, the coalescence of the droplets was at the origin of the coarser observed morphologies. The evolution from a nodular morphology to a fibrillar one with increasing glycerol content was already demonstrated in PE/starch blends by Rodriguez-Gonzales et al.[6] and was explained by the viscosity ratio. In the case of TPF A, the drop in the viscosity ratio with increasing glycerol content explained the formation of a more elongated dispersed phase, which was favorable for the formation of a cocontinuous morphology, as shown in Figure 5(c).[48]

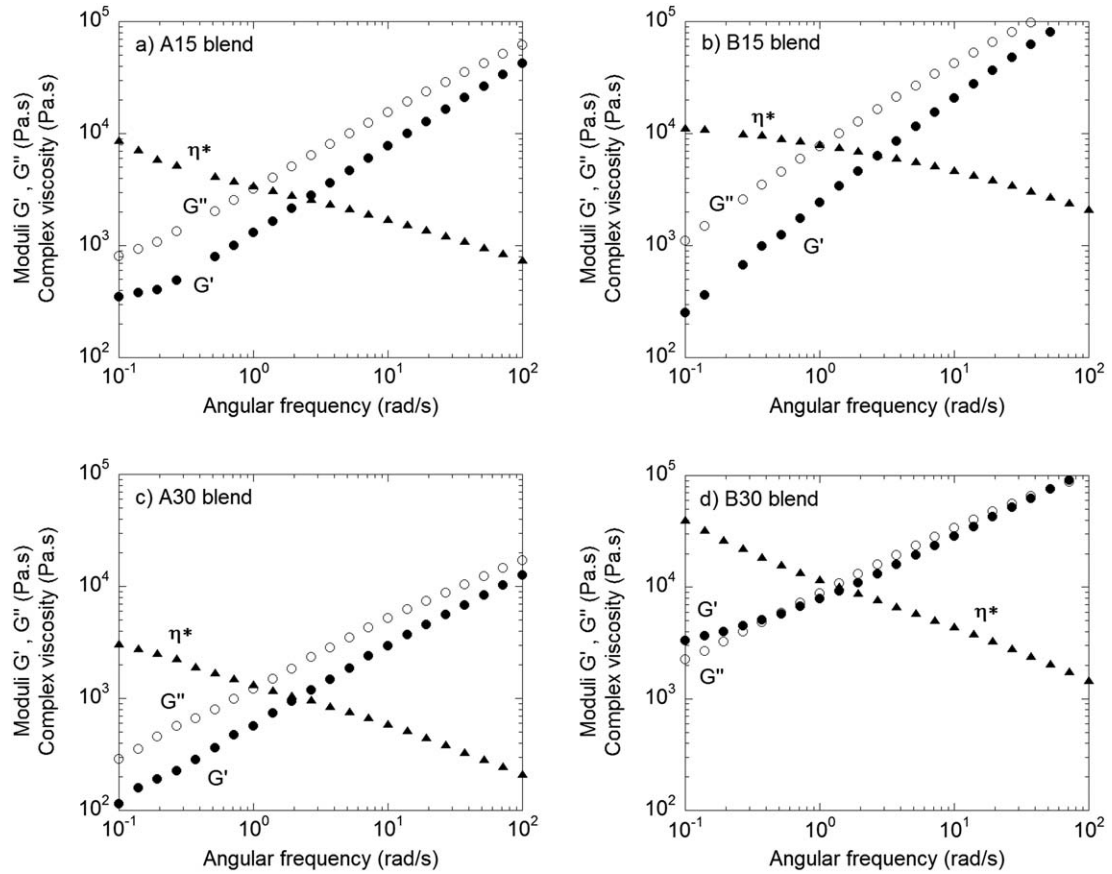

Figure 8. Rheological response of the TPF/PBAT blends (G', G'', and η^* vs the frequency): (a) A15 blend, (b) B15 blend, (c) A30 blend, and (d) B30 blend.

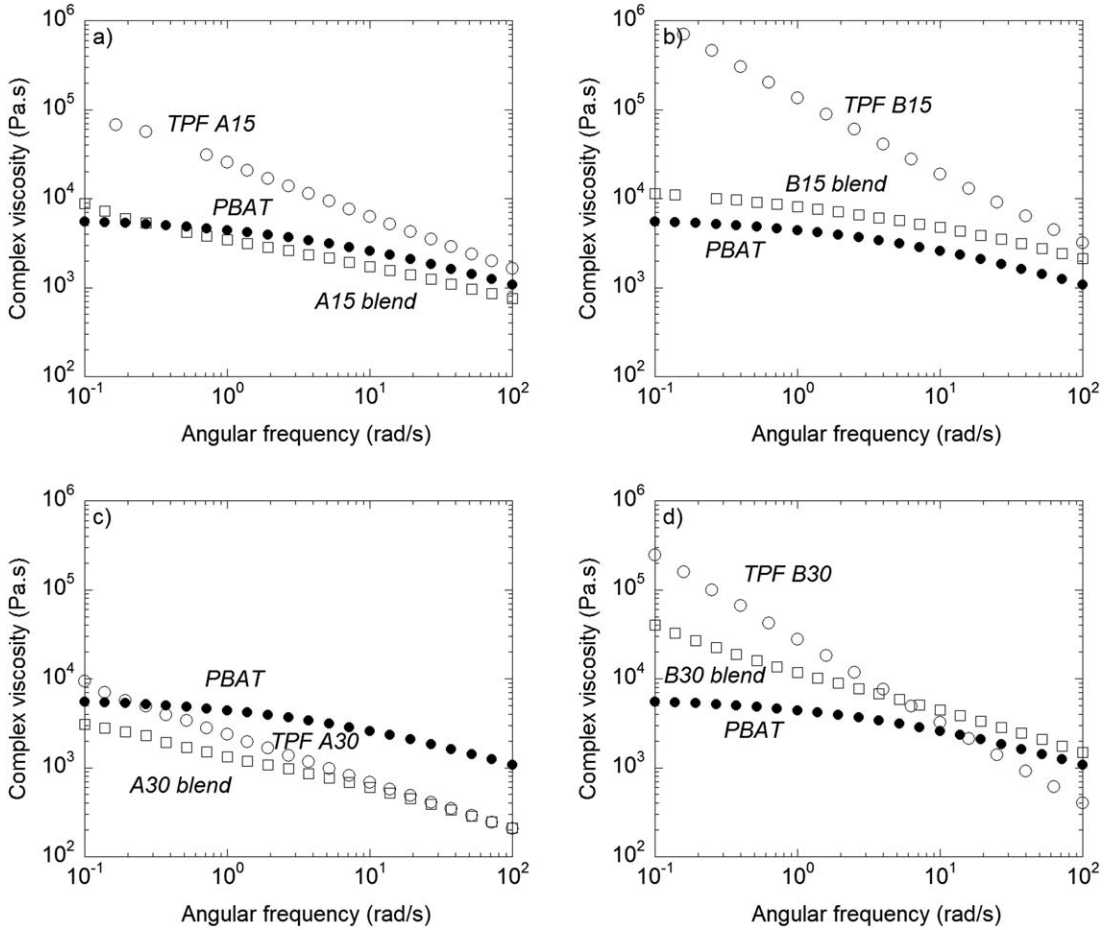

Figure 9. η^* as a function of the frequency at 150°C at 1% strain for the (○) TPF, (●) PBAT, and (□) TPF/PBAT blends: (a) A15, (b) B15, (c) A30, and (d) B30.

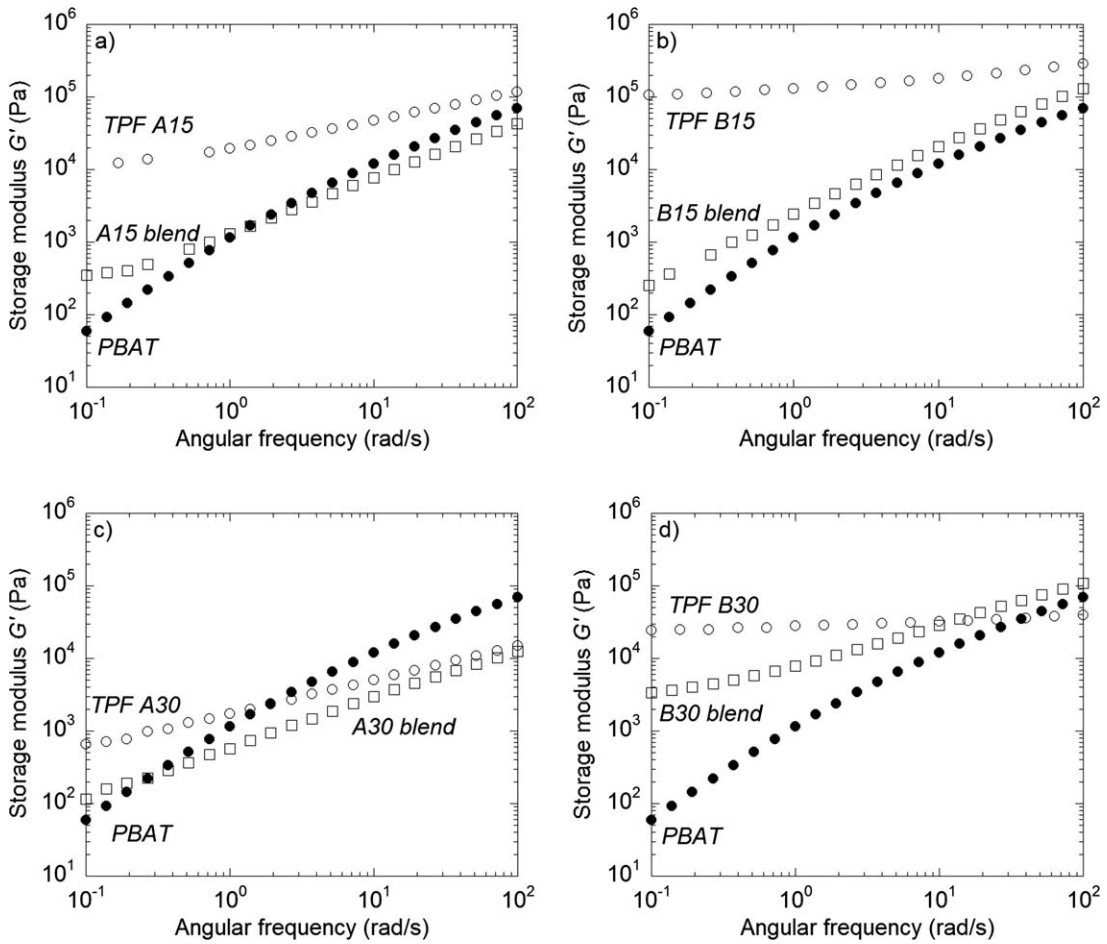

Figure 10. G' as a function of the frequency at 150°C and 1% strain for the (○) TPF, (●) PBAT, and (□) TPF/PBAT blends: (a) A15, (b) B15, (c) A30, and (d) B30.

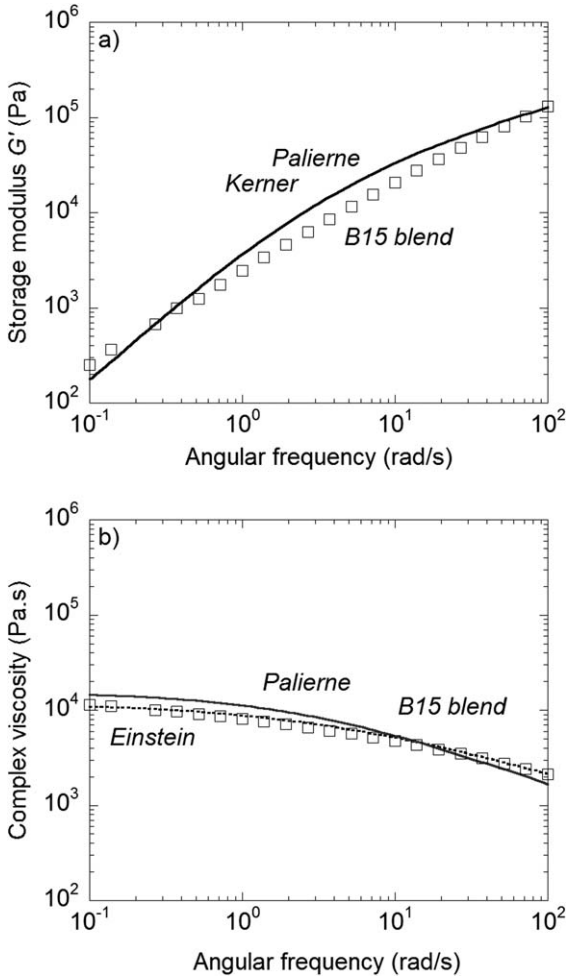

Figure 11. Comparison of the model predictions and experimental measurements for the B15 blend: (a) G' and (b) viscosity. The symbols are experimental values. The lines were obtained with (—) the Palierne model, (- - -) the Kerner model, and (· · ·) the Einstein model.

TPF/PBAT Blend Rheological Behavior

The rheological behavior of each blend at 150°C is compared to that of its respective components (PBAT and TPF) in Figure 9 (η^*) and Figure 10 (G').

With a blend of two immiscible polymers and with the application of a simple mixing rule without interfacial tension (e.g., the model of Kerner[49]), one expects that the modulus or the viscosity should lie between those of the components. The droplet interface (characterized by a specific time relaxation) should give rise to an additional viscoelastic contribution, characterized by a shoulder on the G' curve at intermediate frequency, which could be predicted by the model of Palierne.[50].

The B15 blend G' and viscosity curves tended to follow the tendency of a mixing rule; the B15 blend curves followed the PBAT ones but shifted to higher values. The B30 blend also followed the matrix behavior but with a pronounced departure at a low frequency. The A15 blend followed more closely the behavior of TPF A15 than that of PBAT but with values inferior to the ones of both components. This was similar for the A30 blend, which exhibited a cocontinuous morphology.

An attempt was made to interpret the B15 blend data with classical blend models (Kerner and Palierne). The droplet size was taken to have a 1 μm radius (as observed by SEM), and for the Palierne model, the interfacial tension was varied in the usual range, that is, between 1 and 15 mN/m. The experimental curves for the blend B15 [Figure 11(a)] were globally fitted by the two models. However, the calculations did not show any difference between the simple mixing rule and the Palierne model, whatever the range of droplet size and interfacial tension. Because of the high viscosity and elasticity of TPF B15 relative to those of PBAT, the inclusions did not seem to be deformed during the solicitation. For this reason, the B15 blend was considered as a suspension. A suspension model, such as the Krieger–Dougherty model, for example, predicts that the suspension Newtonian viscosity is equal to that of the matrix multiplied by a constant factor depending on the volume fraction and close packing fraction. The viscosity curve of the suspension should thus be parallel to that of the matrix in a log–log representation. This effectively corresponded to the behavior of the B15 blend, as shown in Figure 9(b). As shown in Figure 11(b), this behavior could be nicely described by the simple Einstein equation.

The B30 blend [Figures 9(d) and 10(d)] showed a similar rheological response, except at low frequency with the presence of an onset of a G' plateau; this indicated the existence of a melt yield stress. This indicated that interactions between particles were eventually favored compared to B15 by the smaller particle size. This also confirmed that these blends behaved more like suspensions with a solid TPF phase than like classical blends.

The A15 and A30 blends displayed behavior closer to that of the TPFs. For these materials, the TPF viscosity was closer or even lower than that of PBAT. The morphology was nodular with large nodules (the A15 blend) or cocontinuous (the A30 blend). Consequently, the influence of the TPF phase was more pronounced.

Anyway, it seems very difficult to propose clear explanations for these various results: the behavior of the components, together with the blend morphology, did not allow a correct interpretation. Moreover, it is worth pointing out that the evolution of the volume fraction of the TPS phase via the evaporation of plasticizer during the mixing process could not be neglected.

CONCLUSIONS

We studied the behavior of two flours plasticized with two glycerol contents in an internal mixer and then blended them with a PBAT matrix under identical conditions. The rheological study of the TPFs highlighted two different behaviors. In the case of the waxy-grade flour, we observed the behavior of a high molecular weight viscoelastic polymer, and in the case of the standard grade flour, we observed a gel-like behavior. In all cases, the glycerol content only modified the viscosity level. The water content, which decreased considerably during mixing, also influenced the TPF viscosity.

The study showed that the TPF rheological behavior governed the blends' morphologies and their rheological behavior. The

TPF rheological behavior was governed by the flour nature, that is, the amylose/amylopectin ratio and the plasticizer content, in a similar way as that for TPS. According to the amylose/amylopectin ratio and plasticizer content, different morphologies and sizes of the starchy phase were obtained. The glycerol content modified the viscosity ratio between the TPF and PBAT matrix and, thus, the ability of the TPF particles (or droplets) to deform and break or to coalesce to form a cocontinuous phase. The development of a cocontinuous structure appeared to be due to the behavior, size, and shape of the particles rather than the viscosity ratio of the two phases. Indeed, a gel-like behavior of the dispersed phase seemed to prevent the coalescence of droplets or fibrils and allowed for much finer structures. Through the selection of the flour type, plasticizer amount, and mixing conditions (not presented here), it is thus possible to obtain blends with a wide variety of morphologies and rheological properties; this will lead to final products with various possible applications. The use of TPF in bioplastic blends may constitute interesting alternatives to TPS with an economic interest. Flour is less expensive than starch because of its simpler process of obtention.

ACKNOWLEDGMENTS

This study was conducted as part of the French project called CEREMAT, which was supported by the Cereales Vallée cluster. The authors gratefully thank Fond Unique Interministériel for its financial support, the project members for their permission to publish this article, and Ecole Nationale Supérieure de Chimie de Clermont-Ferrand (France) for the measurements of the glycerol content in the TPFs and their blends.

REFERENCES

1. Griffin, G. J. L. *Polym. Degrad. Stab.* **1994**, *45*, 241.
2. Yu, L.; Dean, K.; Li, L. *Prog. Polym. Sci.* **2006**, *31*, 576.
3. Wang, X. L.; Yang, K. K.; Wang, Y. Z. *J. Macromol. Sci.* **2003**, *43*, 385.
4. Lu, D. R.; Xiao, C. M.; Xu, S. *J. Express Polym. Lett.* **2009**, *3*, 366.
5. St-Pierre, N.; Favis, B. D.; Ramsay, B. A.; Ramsay, J. A.; Verhoogt, H. *Polymer* **1997**, *38*, 647.
6. Rodriguez-Gonzalez, F. J.; Ramsay, B. A.; Favis, B. D. *Polymer* **2003**, *44*, 1517.
7. Fu, X.; Chen, X.; Wen, R.; He, X.; Shang, X.; Liao, Z.; Yang, L. *J. Polym. Res.* **2007**, *14*, 297.
8. Walker, A. M.; Tao, Y.; Torkelson, J. M. *Polymer* **2007**, *48*, 1066.
9. Thakore, I. M.; Desai, S.; Sarawade, B. D.; Devi, S. *Eur. Polym. J.* **2005**, *37*, 151.
10. Vinhas, G. M.; Moreira de Lima, S.; Santos, L. A.; Gomes de Andrade Lima, M. A.; Bastos de Almeida, Y. M. *Braz. Arch. Biol. Technol.* **2007**, *50*, 361.
11. Landreau, E.; Tighzert, L.; Bliard, C.; Berzin, F.; Lacoste, C. *Eur. Polym. J.* **2009**, *45*, 2609.
12. Teyssandier, F.; Cassagnau, P.; Gérard, J. F.; Mignard, N. *Eur. Polym. J.* **2011**, *47*, 2361.
13. Huneault, M. A.; Li, H. *Polymer* **2007**, *48*, 270.
14. Jang, W. Y.; Shin, B. Y.; Lee, T. J.; Narayan, R. *J. Ind. Eng. Chem.* **2007**, *13*, 547.
15. Jun, C. L. *J. Polym. Environ.* **2000**, *8*, 33.
16. Sarazin, P.; Li, G.; Orts, W. J.; Favis, B. D. *Polymer* **2008**, *49*, 599.
17. Arroyo, O. H.; Huneault, M. A.; Favis, B. D.; Bureau, M. N. *Polym. Compos.* **2010**, *31*, 114.
18. Averous, L.; Moro, L.; Dole, P.; Fringant, C. *Polymer* **2000**, *41*, 4157.
19. Rosa, D. S.; Guedes, C. G. F.; Pedroso, A. G.; Calil, M. R. *Mater. Sci. Eng. C* **2004**, *24*, 663.
20. Matzinos, P.; Tserki, V.; Kontoyiannis, A.; Panayiotou, C. *Polym. Degrad. Stab.* **2002**, *77*, 17.
21. Li, G.; Favis, B. D. *Macromol. Chem. Phys.* **2010**, *211*, 321.
22. Bossard, F.; Pillin, I.; Aubry, T.; Grohens, Y. *Polym. Eng. Sci.* **2008**, *48*, 1862.
23. Nayak, S. K. *Polym. Plast. Technol. Eng.* **2010**, *49*, 1406.
24. Schwach, E.; Averous, L. *Polym. Int.* **2004**, *53*, 2115.
25. Ren, J.; Fu, H. Y.; Ren, T. B.; Yuan, W. Z. *Carbohydr. Polym.* **2009**, *77*, 576.
26. Nabar, Y.; Raquez, J. M.; Dubois, P.; Narayan, R. *Biomacromolecules* **2006**, *6*, 807.
27. Ratto, J. A.; Stenhouse, P. J.; Auerbach, A.; Mitchell, J.; Farrell, R. *Polymer* **1999**, *40*, 6777.
28. Mani, R.; Bhattacharya, M. *Eur. Polym. J.* **2001**, *37*, 515.
29. Willette, J. L.; Shogren, R. L. *Polymer* **2002**, *43*, 5935.
30. Vargha, V.; Truter, P. *Eur. Polym. J.* **2005**, *41*, 715.
31. Utracki, L. A. Polymer Blends Handbook; Kluwer Academic: Dordrecht, The Netherlands, **2002**.
32. Isayev, A. I. Encyclopedia of Polymer Blends; Wiley-VCH: New York, **2010**.
33. Tester, R. F.; Karkalas, J. In Biopolymers; De Baets, S., Vandamme, E., Steinbuchel, A., Eds.; Wiley-VCH: Weinheim, **2002**; Vol. *6*, p 381.
34. Della Valle, G.; Buléon, A.; Carreau, P. J.; Lavoie, P. A.; Vergnes, B. *J. Rheol.* **1998**, *42*, 507.
35. Della Valle, G.; Colonna, P.; Patria, A.; Vergnes, B. *J. Rheol.* **1996**, *40*, 347.
36. Della Valle, G.; Vergnes, B.; Lourdin, D. *Int. Polym. Proc.* **2007**, *12*, 471.
37. Willett, J. L.; Jasberg, B. K.; Swanson, C. L. *Polym. Eng. Sci.* **1995**, *35*, 202.
38. Tajuddin, S.; Xie, F. W.; Nicholson, T. M.; Liu, P.; Halley, P. *J. Carbohydr. Polym.* **2011**, *83*, 914.
39. Van Soest, J. J. G.; Hulleman, S. H. D.; de Wit, D.; Vliegenthart, J. F. G. *Ind. Crops Prod.* **1996**, *5*, 11.
40. Colonna, P.; Mercier, C. *Carbohydr. Polym.* **1983**, *3*, 87.

41. Yang, Q.; Chung, T. S.; Weber, M.; Wollny, K. *Polymer* **2009**, *50*, 524.
42. McKee, M. G.; Unal, S.; Wilkes, G. L.; Long, T. E. *Prog. Polym. Sci.* **2005**, *30*, 507.
43. Wu, S. *Polym. Eng. Sci.* **1987**, *27*, 335.
44. Grace, H. P. *Chem. Eng. Commun.* **1982**, *14*, 225.
45. Serpe, G.; Jarrin, J.; Dawans, F. *Polym. Eng. Sci.* **1990**, *30*, 553.
46. Bousmina, M.; Ait-Kadi, A.; Faisant, F. B. *J. Rheol.* **1999**, *43*, 415.
47. Brouillet-Fourmann, S.; Carrot, C.; Mignard, N.; Prochazka, F. *Appl. Rheol.* **2000**, *12*, 192.
48. Willemse, R. C.; Posthuma de Boer, A.; van Dam, J.; Gotsis, A. D. *Polymer* **1998**, *39*, 5879.
49. Kerner, E. H. *Proc. Phys. Soc. London B* **1956**, *69*, 808.
50. Palierne, J. F. *Rheol. Acta* **1990**, *29*, 204.